International Journal of Thermophysics, Vol. 25, No. 5, September 2004 (© 2004)

Effect of Porosity on Thermal Conductivity of Al–Si–Fe–X Alloy Powder Compacts[1]

K. Y. Sastry,[2,3] L. Froyen,[2] J. Vleugels,[2] E. H. Bentefour,[4] and C. Glorieux[4,5]

The thermal conductivity and thermal diffusivity of hot- and cold-pressed Al–17Si–5Fe–3.5Cu–1.1Mg–0.6Zr (mass%) alloy powder compacts were investigated as a function of the porosity volume fraction. Samples with a very low degree of porosity were produced by hot-pressing air atomized alloy powder with a particle size of 45–100 μm. The same powder was used to produce highly porous compacts by cold compaction using a manual press. The thermal diffusivity of the powder compacts was measured using a sinusoidal modulation photopyroelectric technique in a configuration that is similar to the laser flash method. The thermal diffusivity of the material decreases by a factor of about 13 with an increasing porosity of 25 vol% and a factor of about 300 at 60 vol % porosity. Since the calculated specific heat (weighted average of mass specific heat values of major alloy compounds) is much less porosity dependent, the porosity dependence of the thermal conductivity is similar to the thermal diffusivity and decreases exponentially with increasing porosity. Microstructural characterization of high porosity samples prepared by cold compaction indicated that the distribution of pores is not uniform over the cross-section. An interconnecting network of open and closed pores in the form of channels created pockets of porosity,

[1]Paper presented at the Fifteenth Symposium on Thermophysical Properties, June 22–27, 2003, Boulder, Colorado, USA.

[2]Department of Metallurgy and Materials Engineering (MTM), Katholieke Universiteit Leuven (K.U. Leuven), Kasteelpark Arenberg 44, B-3001 Leuven, Belgium.

[3]To whom correspondence should be addressed. E-mail: sastry.kandukuriyagnanna@mtm.kuleuven.ac.be

[4]Laboratory for Acoustics and Thermal Physics (ATF), Department of Physics, Katholieke Universiteit Leuven (K.U. Leuven), Celestijnenlaan 200D, B-3001 Leuven, Belgium.

[5]Postdoctoral Researcher with Fonds voor Wetenschappelijk Onderzoek–Vlaanderen (FWO-V), Egmontstraat 5, B-1000 Brussels, Belgium.

0195-928X/04/0900-1611/0

which are largely responsible for a drastic reduction of thermal conductivity with increasing porosity.

KEY WORDS: Al–Si–Fe–X alloy; porosity; powder; thermal conductivity; thermal diffusivity.

1. INTRODUCTION

Powder metallurgy (P/M) concerns the production of densified materials from elemental or prealloyed powder in such a way that the densified material has the desired properties and shape. Very often, P/M is the only production route to make a certain material with demanding properties as, for example, highly alloyed metals with very fine and homogeneous microstructure. Hypereutectic powder metallurgical Al–Si–Fe–X alloys are such materials with good mechanical properties up to elevated temperatures, high wear resistance, a low coefficient of thermal expansion, and good thermal stability. Hence, they are very attractive for applications in the transportation sector, such as the cyclic moving components in a car engine [1].

It is impossible to create new material classes, design different products, and simulate their thermal conditions without a proper knowledge of the thermal properties. With powder compaction methods such as hot pressing, hot isostatic pressing, extrusion, and field-assisted sintering processes, the density of the powder increases with the applied loads and dwell time. In order to model such densification phenomena, reliable material data on the porosity dependence of thermal properties of the material under study is an essential requirement to achieve successful results [2–6]. Although many models for the porosity dependence of physical properties for ceramics and other materials have been derived in the past, the available database and models are often inadequate to quantitatively predict the thermal properties for many powder systems of practical interest [7].

The main aim of this work is to investigate the porosity dependence of the thermal properties of a multicomponent Al–Si–Fe–X complex alloy, which is a typical example of prominent industrial importance.

2. EXPERIMENTAL

2.1. Method and Material

The photopyroelectric (PPE) technique has been used to determine the thermal diffusivity of prealloyed Al–17Si–5Fe–3.5Cu–1.1Mg–0.6Zr (mass%) powder compacts of various densities. To prepare samples with

a wide porosity range from 0 to 60 vol.%, different compaction methods were used. Porous compacts with a high amount of porosity were compacted by cold compaction using a manual press with relatively low applied loads. Very low porosity levels of 0.4 and 1.8 vol.% were produced by hot pressing under vacuum in steel dies at different applied mechanical loads and at elevated temperature. Spray compaction and extrusion steps were followed to produce non-porous samples. Density measurements were carried out in ethanol according to the Archimedes principle (BP210S balance, Sartorius AG, Germany). The measurement of the thermal diffusivity of a series of samples with varying porosity was performed at room temperature ($\sim$20 °C). At least 10 measurements were performed on each sample. The measurement time was around 90 min for each measurement. A careful calibration of the experimental setup and procedure was performed and verified by measuring the thermal diffusivity of an aluminum sample of known diffusivity, prior to carrying out the actual measurements.

2.2. Experimental Technique

The photopyroelectric (PPE) technique involves the detection (via a pyroelectric sensor) of the temperature rise in a sample exposed to an intensity-modulated beam of laser light. The absorbed light is converted into heat, which gives rise to periodic temperature variations. The generated thermal waves propagate through the sample and are detected by the pyroelectric detector, which is very sensitive to even very small changes in the heat flux. The detected signal current is proportional to the rate of temperature change [8,9]. The thermal diffusivity is a quantity that plays an essential role in the temperature response of materials that are dynamically heated (e.g., pulsed or sinusoidally modulated). It expresses the rate of transfer of temperature modulations. The thermal conductivity appears in situations of quasi-steady state temperature profiles, and is related to the magnitude of a heat flux resulting from a given temperature gradient.

2.3. Experimental Setup

The schematic diagram of the PPE cell is shown in Fig. 1. The pyroelectric sensor (300 μm thick, 15 $\times$ 15 mm^2 z-cut lithium tantalate crystal) is mounted on a ring in an electromagnetically shielded cell. A 20 mW He–Ne laser (Uniphase) with a wavelength of 632.8 nm, intensity modulated by an acousto-optic modulator, is used as an optical heating source. A sample of Ø10 mm is placed on the pyroelectric detector and is thermally coupled by means of a thin layer of an oil-based compound whose

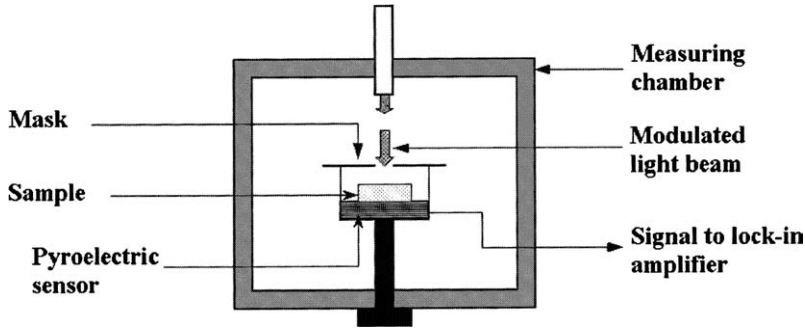

Fig. 1. Schematic diagram of the PPE cell setup used for measuring thermal diffusivity.

contribution to the attenuation of the transmitted thermal wave signal is incorporated in the calculations of thermal diffusivity. An optical mask placed on top of the sample prevents light to directly strike the sensor. In that way, all generated heat has to pass the sample before reaching the detector.

The signal output, i.e., the current generated by the sensor and collected by two electrodes, is measured with a lock-in amplifier (Stanford SR-830). The operating parameters are controlled through a computer equipped with adapted virtual instrument software allowing automatic data acquisition. The frequency range for the scan was 0.05–10.000 Hz.

In the low frequency modulated radiation regime, the thermal wave penetrates deep into the sample and reaches the sensor, resulting in a dominant and useful contribution to the pyroelectric signal. With increasing modulation frequency, f, the sample becomes thermally thick and the pyroelectric signal $S(f)$ decreases exponentially. The decay rate is determined by the sample thickness, d, and the thermal diffusivity, α, of the sample.

$$S(f) = S_0 \exp\left(-(1+i)\sqrt{\frac{\pi f}{\alpha}}d\right) \tag{1}$$

$$\ln|(S)| = \ln|(S_0)| - \sqrt{\frac{\pi}{\alpha}}d\sqrt{f} \tag{2}$$

$$\phi_S = \phi_{S_0} - \sqrt{\frac{\pi}{\alpha}}d\sqrt{f} \tag{3}$$

where $i = \sqrt{-1}$ is the imaginary unit, $S(f)$ is the complex PPE signal, S and ϕ_S are its amplitude and phase factors, respectively. Equations (1)–(3)

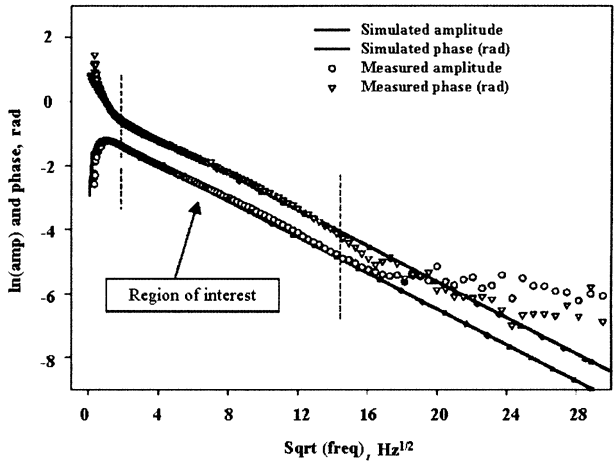

Fig. 2. Typical output of experimental data from thermal diffusivity measurements represented as Sqrt (freq) vs. ln (amp) and phase (rad) components of complex PPE signal in comparison to the simulated model.

indicate that a frequency scan of the phase of the PPE signal provides a direct and absolute measurement of the sample's thermal diffusivity [10].

Figure 2 shows an acquired pyroelectric signal, plotted as the square root (Sqrt) of the frequency vs. the natural logarithm of the amplitude component and the Sqrt of the frequency vs. the phase (rad) component of the complex PPE signal. In the useful frequency range, in both cases the curve is linear with a slope $s = \sqrt{\frac{\pi}{\alpha}} d$, which depends on the sample diffusivity, α_S, and thickness, d_S. At very high frequencies, the thermal signal contribution disappears and the signal becomes dominated by piezoelectrically detected signal contributions and electromagnetic pickup. This anomalous signal is very small and rather frequency independent.

2.4. Determination of Thermal Conductivity

The thermal conductivity (λ) is calculated from the thermal diffusivity as follows:

$$\lambda = \alpha C_p \rho \tag{4}$$

C_p is the specific heat capacity, and ρ is the density of the sample. As no specific heat capacity measurement was performed in the present study, C_p was calculated as a weighted sum of the individual heat capacities

of the major alloying elements in conjunction with the Neumann–Kopp rule. Minor alloying elements were not taken into account in the heat capacity estimation, because the material is a prealloyed powder with a homogeneous microstructure and not a mechanical mixture of constituent elements.

3. RESULTS AND DISCUSSION

The investigated samples are described in Table I. The theoretical density of the Al–17Si–5Fe–3.5Cu–1.1Mg–0.6Zr (mass%) alloy is normally in the range of 2840–2860 $kg \cdot m^{-3}$ depending on the actual chemical composition of the powder. In the present study, a value of 2840 $kg \cdot m^{-3}$ for the density of the fully dense material is used as a reference value to calculate the relative density of the samples. Porosity values are obtained by deducting the calculated values of percentage theoretical density from 100. Porosity values calculated as described above are the sum of open and closed porosities present in the sample. It is noteworthy to mention here that although the porosity in the hot-pressed samples is assumed to be uniform, which is not the case for the cold-pressed samples. A multipycnometer (Quantachrome MPV-1) was used to quantify the interconnecting, closed and total porosity in the cold-pressed samples, as summarized in Table II. From Table II, it can be seen that more than 95% of the total porosity in the cold-pressed samples is interconnecting porosity. An interconnecting pore network was also observed using optical microscopy. A micrograph of a cross-sectional view of the sample with 23% porosity is shown in Fig. 3. The brighter areas in Fig. 3 are material whereas the darker areas are pores. From the micrograph, it may be seen that both open and closed pores exist and many are interconnecting to form

Table I. Samples of Different Density used to Determine the Thermal Diffusivity

Sample No.	Density ($kg \cdot m^{-3}$)	Theoretical density (%)	Estimated porosity (%)	Sample size (10^{-3} m)		Remarks
				Ø	Thickness	
1	2840	100.0	0.0	10.0	2.01	Extruded
2	2830	99.6	0.4	10.4	2.20	Hot pressed
3	2790	98.2	1.8	10.4	1.24	Hot pressed
4	2180	76.8	23.2	10.1	1.19	Cold pressed
5	2110	74.3	25.7	10.1	2.50	Cold pressed
6	1950	68.7	31.3	10.1	1.32	Cold pressed
7	1150	40.5	59.5	08.7	1.45	Powder

Table II. Determination of the Amount of Interconnecting Pores in Cold-Pressed Samples

Sample No.	Calculated total porosity (%)	Measured closed porosity (%)	Inter-connecting porosity (%)
A	48.5	1.4	47.1
B	26.7	0.6	26.1
C	21.4	0.8	20.6
D	19.0	0.8	18.2

channels across the thickness of the sample. We have also observed that the microscopic details of all cold pressed samples are similar except for the amount of pores. Figure 3 is representative for the pore network in all cold-pressed samples.

Measured values of thermal diffusivity as a function of percentage of the theoretical bulk density are compiled in Table III. The diffusivity values were calculated from the measured slopes of the linear phase and logarithmic amplitude signal curves versus the square root of the frequency using the following equations:

$$\ln|(S)| = \ln|(S_0)| - \left(\sqrt{\frac{\pi}{\alpha_s}}d_s\sqrt{f} + \sqrt{\frac{\pi}{\alpha_o}}d_0\sqrt{f}\right)$$
$$\equiv \ln|(S_0)| - (s_s + s_o)\sqrt{f} \equiv \ln|(S_0)| - s_A\sqrt{f} \tag{5}$$

$$\phi_S = \phi_{S_0} - \left(\sqrt{\frac{\pi}{\alpha_s}}d_s\sqrt{f} + \sqrt{\frac{\pi}{\alpha_o}}d_0\sqrt{f}\right)$$
$$\equiv \phi_{S_0} - (s_s + s_o)\sqrt{f} \equiv \phi_{S_0} - s_\phi\sqrt{f} \tag{6}$$

where d_S and d_o are the thicknesses of the sample and oil film, respectively. s_s and s_o, the two contributions to the total slope (s_A for amplitude and s_ϕ for phase curve) coming from the sample (thermal diffusivity

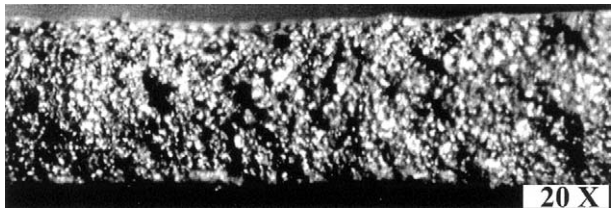

Fig. 3. Micrograph of the sample with 23% porosity showing the network of open and closed pores across the thickness of the sample.

Table III. Experimentally Measured Values of Thermal Diffusivity

Sample No.	Theoretical density (%)	Thermal diffusivity (amplitude) (10^{-6} $m^2 \cdot s^{-1}$)	Thermal diffusivity (phase) (10^{-6} $m^2 \cdot s^{-1}$)	Thermal diffusivity (average) (10^{-6} $m^2 \cdot s^{-1}$)
1	100.0	44.61	46.36	45.49
2	99.6	43.04	36.87	39.96
3	98.2	31.08	31.93	31.51
4	76.8	5.72	5.85	5.79
5	74.3	3.23	3.77	3.50
6	68.7	2.45	2.11	2.28
7	40.5	0.13	0.17	0.15

α_S and thickness d_S) and the coupling fluid (known thermal diffusivity α_o and thickness d_o) are related to the dynamical thermal resistances of these layers in the path of the thermal waves between the excitation region and sensor. The contribution of the oil layer becomes significant for thin samples with low porosity, because in those cases s_o and s_s become comparable. In all experiments, except the one with the 60% porosity sample, there turned out to be an oil film thickness of 20 μm. This value for the thickness was determined from a calibration measurement with a bulk aluminum sample of known thickness and diffusivity. In Fig. 2, the region of interest concerns the low frequency regime where the PPE logarithmic amplitude and phase versus square root of frequency curves are linear and parallel to each other. The diffusivity values obtained from s_A and s_ϕ should be the same. Possible differences indicate the uncertainty of the obtained value. The values reported in Table III are calculated from those measurements where the region of interest is spread over a maximum frequency range. The values obtained from the other measurements are within a 10% range of the reported values. Figure 4 shows a magnified view of the region of interest for the sample with 100% theoretical density.

The calculated specific heat at constant pressure for this alloy is 867 $J \cdot kg^{-1} \cdot K^{-1}$, which is comparable to the measured value reported in the literature[11] for hypereutectic silicon alloys. The average value of the thermal diffusivity, obtained from phase and amplitude signals at each experimental porosity level is used to determine the thermal conductivity (see Table IV). Thermal conductivity values at different porosity levels are shown in Fig. 5. The relation of the thermal conductivity of the Al–17Si–5Fe–3.5Cu–1.1Mg–0.6Zr (mass%) alloy as a function of percent theoretical density is shown graphically in Fig. 6. The linearity of the curve in a semi-logarithmic plot reveals that the thermal conductivity varies expo-

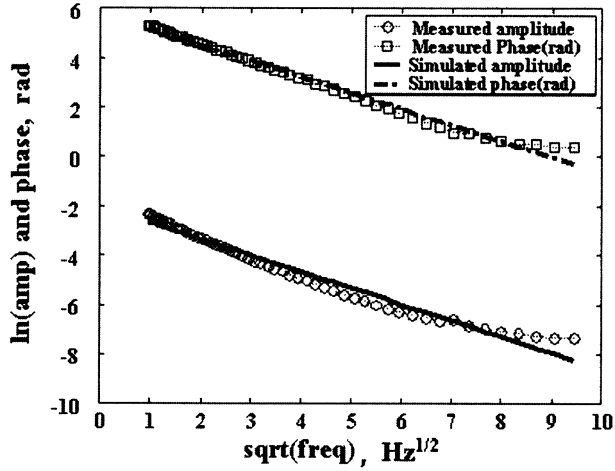

Fig. 4. Experimental and fitted frequency dependence of the amplitude and phase components of the complex photopyroelectric (PPE) signal. The slopes of the curves are equal and determined by the sample thickness and thermal diffusivity. The comparison of the experimental slopes gives a measure for the precision of the derived thermal diffusivity value.

nentially with the percentage of the theoretical density. The experimental data were not consistent with a power law behavior, which is sometimes reported in the literature. The experimental data points were analyzed by calculating the least-squares fit, and the following equation defines the best fit for the thermal conductivity λ vs. percent theoretical density x:

$$\lambda = 0.0025e^{0.1065x} \tag{7}$$

By using this calibration equation, the thermal conductivity for any theoretical density can be calculated. The reported value of thermal conductivity for the fully dense sample may not be taken as an absolute material property. The fully dense sample used in the present study was prepared from spray compaction and extrusion processes. Since the thermal conductivity is also sensitive to the thermal history, it may change when the sample is heat-treated after extrusion. The values reported for each porosity level are reproducible but not absolute values, and they may vary to some extent depending upon the actual alloy composition, powder particle size, densification process, and measuring technique.

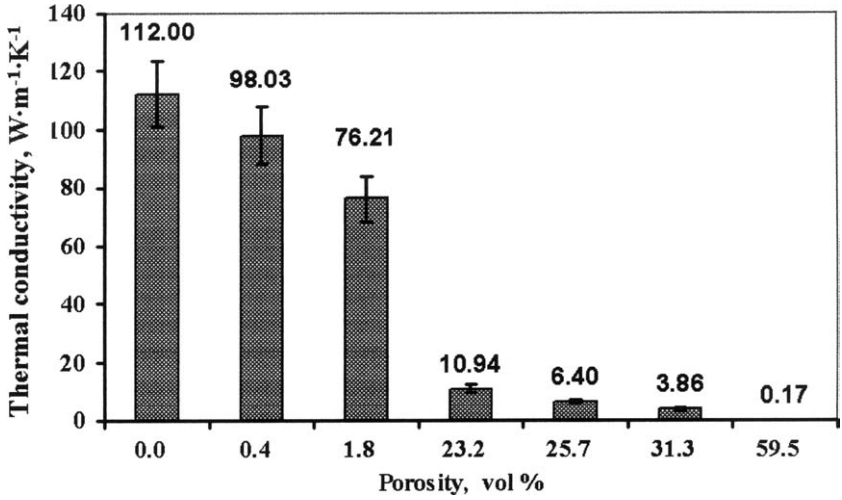

Fig. 5. Calculated values of thermal conductivity of Al–17Si–5Fe–3.5Cu–1.1Mg–0.6Zr (mass%) alloy at different levels of porosity.

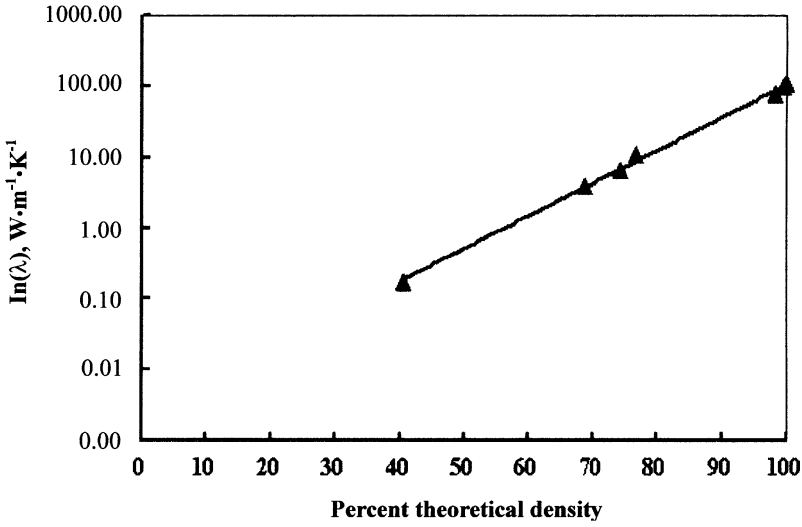

Fig. 6. Porosity dependence of thermal conductivity of Al–17Si–5Fe–3.5Cu–1.1Mg–0.6Zr (mass%) alloy shown as a function of percentage theoretical density measured at room temperature.

Table IV. Determination of Thermal Conductivity

Sample No.	Density ($kg \cdot m^{-3}$)	Thermal diffusivity (average) (10^{-6} $m^2 \cdot s^{-1}$)	Theoretical Density (%)	Thermal conductivity ($W \cdot m^{-1} \cdot K^{-1}$)
1	2840	45.49	100.0	112.00
2	2830	39.96	99.6	98.03
3	2790	31.51	98.2	76.21
4	2180	5.79	76.8	10.94
5	2110	3.50	74.3	6.40
6	1950	2.28	68.7	3.86
7	1150	0.15	40.5	0.17

4. SUMMARY

We have measured the thermal diffusivity of dense and porous Al–17Si–5Fe–3.5Cu–1.1Mg–0.6Zr (mass%) alloy powder compacts at room temperature as a function of the porosity volume fraction in the range of 0–60 vol.%. Air atomized prealloyed powder was shaped into 10 mm diameter round specimens by hot pressing and cold compaction techniques. Microstructural characterization of cold-pressed samples with a high degree of porosity revealed that the distribution of pores across the sample cross-section is not uniform. Clustering of pores and pore network channels are observed which are a representation of the pore distribution during the early stages of powder densification. The thermal conductivity of the specimens was calculated from the measured thermal diffusivity, density, and estimated specific heat. Regression analysis revealed that the thermal conductivity of the alloy increases exponentially with decreasing porosity.

ACKNOWLEDGMENTS

This work was partially supported by the GROWTH program of the Commission of the European Communities under project contract no. G5RD-CT2002–00732. Special thanks to Powder Light Metals GmbH (PLM), Germany for providing the powder and extruded samples.

REFERENCES

1. G. Timmermans, *Direct Powder Forged Hypereutectic Al–Si Alloys*, Ph.D. Thesis, Katholieke Universiteit Leuven, Belgium (2000), pp. 1.1–1.31.

2. A. Bakhshiani, A. R. Khoei, and M. Mofid, *J. Mater. Process. Technol*. **125126:** 138 (2002).
3. C. L. Martin and D. Bouvard, *Acta Mater*. **51**: 373 (2003).
4. M. Galanty, P. Kazanowski, P. Kansuwan, and W. Z. Misiolek, *J. Mater. Process. Technol.***125–126**:491 (2002).
5. O. Yanagisawa, H. Kuramoto, K. Matsugi, and M. Komatsu, *Mater. Sci. Eng. A* **350**:184 (2003).
6. K. A. Khor, K. H. Cheng, L. G. Yu, and F. Boey, *Mater. Sci. Eng. A* **347**:300 (2003).
7. A. Birnboim, T. Olorunyolemi, and Y. Carmel, *J. Am. Ceram. Soc.* **84/6**: 1315 (2001).
8. D. Dadarlat, J. Gibkes, D. Bicanic, and A. Pasca, *J. Food Eng*. **30**:155 (1996).
9. C. Preethy Menon, J. Philip, A. Deepthy, and H. L. Bhat, *Mater. Res. Bull.* **36**:2407 (2001).
10. M. Marinelli, U. Zammit, F. Mercuri, and R. Pizzoferrato, *J. Appl. Phys.***72**:1906 (1992).
11. S. Adolfi, D. M. Jacobson, and A. Ogilvy, *Property Measurements on Osprey Spray-Deposited Al-Si Alloys* (Osprey Metals Ltd., Neath SA11 1NJ, United Kingdom, 2002), pp. 1–14.